Open access • Journal Article • DOI:10.5573/IEIE.2015.52.1.162

Footstep Detection and Classification Algorithms based Seismic Sensor

Youn J. Kang, Jaeil Lee, Jinho Bea, Chong Hyun Lee

Published on: 25 Jan 2015 - Journal of the Institute of Electronics Engineers of Korea (The Institute of Electronics and Information Engineers)

2015년 1월 전자공학회 논문지 제 52권 제 1 호
Journal of The Institute of Electronics and Information Engineers Vol. 52, NO. 1, January 2015 http://dx.doi.org/10.5573/ieie.2015.52.1.162

논문 2015-52-1-19

진동센서 기반 걸음걸이 검출 및 분류 알고리즘

(Footstep Detection and Classification Algorithms based Seismic Sensor)

강 윤 정*, 이 재 일**, 배 진 호***, 이 종 현***

(Youn Joung Kang, Jaeil Lee, Jinho Bea, and Chong Hyun Lee©)

요 약

본 논문에서는 적응형 걸음걸이 검출 알고리즘과 검출된 신호로부터 단일 발자국의 움직임을 분류하는 알고리즘을 제안한다. 제안된 단일 발자국 기반 알고리즘은 기존의 연속된 발자국 신호를 이용한 분류 방식이 아니기 때문에 전체적인 움직임뿐만 아니라 개별적이고 불규칙한 움직임도 검출 및 분류 가능하다. 분류를 위해 사용된 특징벡터는 발자국 신호의 푸리에 스펙트럼, CWT의 스펙트럼, AR 모델링 스펙트럼과 AR 스펙트로그램 영상으로부터 얻어진 벡터이다. SVM을 이용하여 단일 발자국의 움직임을 분류한 결과 AR 스펙트로그램으로 얻어진 특징벡터를 사용할 경우 90% 이상 분류 성능을 얻었다.

Abstract

In this paper, we propose an adaptive detection algorithm of footstep and a classification algorithm for activities of the detected footstep. The proposed algorithm can detect and classify whole movement as well as individual and irregular activities, since it does not use continuous footstep signals which are used by most previous research. For classifying movement, we use feature vectors obtained from frequency spectrum from FFT, CWT, AR model and image of AR spectrogram. With SVM classifier, we obtain classification accuracy of single footstep activities over 90% when feature vectors using AR spectrogram image are used.

Keywords : Single footstep, seismic sensor, adaptive footstep detection, footstep classification

Ⅰ. Introduction

Personnel detection and classification are an important aspect of intelligence, surveillance, and reconnaissance. It plays a vital role in border and camp protection[1~2]. All these applications involve deployment of sensors for a prolonged time; these sensors are often camouflaged so as not to be noticeable by an intruder's visual inspection[3]. Currently, research about multimodal unattended ground sensors (UGS) is being carried to detect and classification target in our country's border[4~5]. These UGSs, once deployed, should operate for a prolonged period of time because of their low power consumption. Some of the sensors that require low power are E-field, acoustic, seismic and magnetic. In most UGSs, the imaging sensors are dormant and

* 학생회원, 한국과학기술원 해양시스템공학전공
(Division of Ocean Systems Engineering, KAIST)
** 학생회원, *** 정회원, 제주대학교 해양시스템공학과
(Dept. of Ocean System Engineering, Jeju Nat'l University)
© Corresponding Author (E-mail: chonglee@jejunu.ac.kr)
※ This research was supported by the 2014 scientific promotion program funded by Jeju National University
접수일자: 2014년07월28일, 수정일자: 2014년12월09일
게재확정: 2014년12월30일

only wake up to take a picture once the non-imaging sensors determine that there is a viable human target present in the vicinity.

Personnel detection and classification using seismic sensors has been considered by several authors in the literature. Seismic sensors are small enough that they can be easily hidden away so as to not be noticeable from an intruder's visual inspection. Moreover, the creation of artificial vibrations intended to cause confusion in the recognition process is very difficult. Primarily, the seismic sensors are used to estimate the cadence of a person walking[6~8]. Bland has discussed the use of autoregressive coefficients in designing a footstep detection scheme from acoustic and seismic sensors[9]. Succi et al. proposed the use of signal kurtosis as a test statistic for detection of human footstep signals[10]. Park et al. have considered the problem of detecting and classifying perimeter intrusion using geophones[11]. Iyengar et al. fused acoustic and seismic signals for footstep detection[12]. Their work discusses a novel approach based on canonical correlation analysis and copula theory to establish a likelihood ratio test. Houston and McGaffigan have proposed using cadence features for detection of footsteps[7].

All of the mentioned research have used the fundamental gait frequency, interval of cadence and amplitude of signal. Thus, they can not detect movement when footstep intervals are the same.

To overcome this problem, we propose an adaptive detection algorithm and a classification algorithm based on single footstep. Unlike the previous research, the proposed algorithm can classify each footstep movement regardless of gait frequency and cadence interval.

This paper is organized as follows: In Section II, we describe the seismic signal dataset collected by the authors' group and extract the footsteps from the signal. Section III describes the feature extraction based on frequency spectrum and AR spectrogram for classification. We demonstrate experimental results in Section IV by using support vector machine(SVM). Section V concludes the paper with a brief summary and discussion.

Ⅱ. Adaptive footstep Detection

When humans walk or run, the footsteps generate impulsive seismic signals that propagate through the earth surface. The average speed of the seismic signal was measured as 252.6 m/s, by using Rayleigh wave propagation[4]. Geophones are used to capture signals generated by these waves. We recorded the seismic data generated by the footsteps of the walking and running human using GS 11D seismic sensor(OYO Geospace company). The layout of the sensors deployed and the path trajectory of the human is shown in Fig. 1. The target is moving in the direction of the random and the distance between the target and the sensor is 2 ~ 8.2m. Data is obtained from three persons of which heights and weights are summarized in Table1. Then, each person walks and runs according to the given movement scenario.

The received seismic signal has different amplitude and period due to the type of target, how the target is moving(walking, running) and depending on the distance between the target and the sensor. We may can classify the target and activities using cadence, peak amplitude and span of the signal if distance

표 1. 개인 신체 정보
Table 1. Personal physical information.

	H1	H2	H3
hight(cm)	168	171	172
weight(kg)	78	79	70

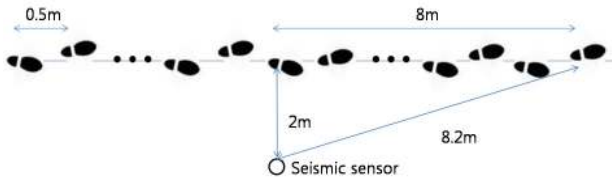

그림 1. 데이터 수집 시나리오
Fig. 1. Data collection scenario.

between the target and sensor is constant. It is difficult to classify the object using only the seismic amplitude, when distance information between the target and the sensor is absent.

The received seismic signal has periodic characteristics by the continuity of the gait, i.e. the period when human is running is shorter than when human is walking. However, classification result depend on the behavior of the target's gait, targets walking quickly and slowly running cannot be classified. In addition, activity which is mixed human walk and run cannot be classified because the period is not constant. In this paper, we extract the single footstep from the seismic signal and classify the target activities using the footstep characteristics.

Predicting performance under operational conditions add additional complexity due to wide variation in target and noise statistics. Especially, performance of the seismic sensor depends on the characteristic of background noise. If statistics of background noise are not time-varying, the threshold V_T maintains the specified probability of false alarm. However, statistics of background noise depend on the component of soil. Even the same location, hence the same soil component, the noise statistics vary with temperature and humidity of the soil and even the air[5]. In order to maintain a constant probability of false alarm in the presence of non-stationary noise, an adaptive threshold method is required.

Signal detection is a classical problem of binary hypothesis testing. Under the null hypothesis H_0, the received signal $y(t)$ is composed of noise alone. The background noise is the random Gaussian distribution in seismic sensor, and the envelope of the random Gaussian noise is Rayleigh distribution.

$H_0 : y(t) = n(t)$ where $n(t) \sim N(0, \sigma_0^2)$

$$p_{X|H_0}(x|H_0) = \frac{x}{\sigma_0^2} exp\left[-\frac{x^2}{2\sigma_0^2}\right] \quad (1)$$

where σ_0^2 is the conditional variance and $p_{X|H_0}(x|H_0)$ is the conditional probability density function of given that the envelope of received signal, and the signal is only noise. Eq. (1) depends on the signal parameter σ_0^2.

Under hypothesis H_1, the received signal $y(t)$ is the sum of the transmitted signal and noise. In the footstep signal, there are the noise $n(t)$ and the signal $s(t)$. The noise and signal are the random Gaussian distribution in the seismic sensor. If both random signals n(t) and s(t) are statistically independent Gaussian distributed with the same zero mean and the different variance (σ_0^2, σ_1^2), then the variance of their sum equals the sum of their variance, i.e., if $n(t) \sim N(0, \sigma_0^2)$ and $s(t) \sim N(0, \sigma_1^2)$ then

$H_1 : y(t) = s(t) + n(t)$

$$p_{X|H_1}(x|H_1) = \frac{x}{\sigma^2} \exp\left(-\frac{x^2}{2\sigma^2}\right) \quad (2)$$

where $y(t) = n(t) + s(t) \sim N(0, \sigma_0^2 + \sigma_1^2) \sim N(0, \sigma^2)$, σ^2 is the conditional variance and $p_{X|H_1}(x|H_1)$ is the conditional probability density function of X given that the received signal is a random signal plus noise. Fig. 2 indicates the histogram and the probability density functions under H_0 and H_1.

The detection threshold level is calculated using Neyman-Pearson detection criterion and distribution parameter of noise. The threshold is obtained once

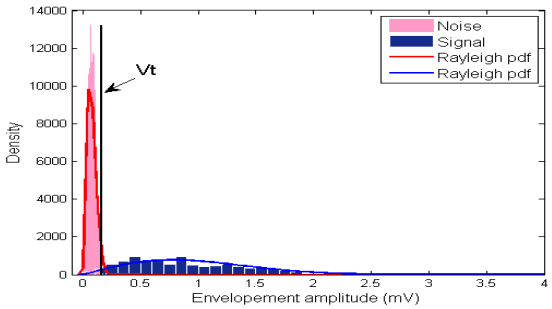

그림 2. 신호와 잡음의 히스토그램 및 레일리 확률밀도 함수 회귀분석

Fig. 2. Histogram and Rayleigh pdf fitting of noise and signal.

the probability of false alarm is set. Fig. 2 shows the distributions of noise and signal using collected data. As seen in Fig. 2, the probability of false alarm is the area under the pdf of background noise above the threshold level V_T.

$$P_{FA} = \int_{x=V_T}^{\infty} p_{X|H_0}(x|H_0)\,dx = \int_{x=V_T}^{\infty} \frac{x}{\sigma_0^2}\exp\left(-\frac{x^2}{2\sigma_0^2}\right)dx = \exp\left(-\frac{V_T^2}{2\sigma_0^2}\right) \quad (3)$$

solving for V_T yields

$$V_T = \sigma_0\sqrt{-2\ln P_{FA}} \quad (4)$$

where σ_0 is the scale parameter of the noise distribution. For example, under 10% of P_{FA}, the threshold voltage is $V_T = 2.146\,\sigma_0$.

As shown in Fig. 2, the probability of detection is the area under the signal-plus-noise curve above the detection threshold.

$$P_D = \int_{x=V_T}^{\infty} p_{X|H_1}(x|H_1)\,dx = \int_{x=V_T}^{\infty} \frac{x}{\sigma^2}\exp\left(-\frac{x^2}{2\sigma^2}\right)dx = \exp\left(-\frac{V_T^2}{2\sigma^2}\right) \quad (5)$$

where $\sigma^2 = \sigma_0^2 + \sigma_1^2$, σ_0^2 is the variance of the noise and σ_1^2 is the variance of the signal.

The receiver operating characteristic(ROC) curve is also known as a relative operating characteristic curve, because it is a comparison of two operating characteristics (P_D and P_{FA}) as the criterion changes [13]. As shown in Fig. 2, the probability of detection is the area under the signal-plus-noise curve above the detection threshold, and the probability of false alarm is the area under the noise-only curve above the threshold level V_T. Using Eq. (3) and Eq. (5), P_D and P_{FA} are present as Eq. (6).

$$P_D(\gamma) = (\alpha^2\gamma)^{-\frac{1}{\alpha^2-1}}$$
$$P_{FA}(\gamma) = (\alpha^2\gamma)^{-\frac{\alpha^2}{\alpha^2-1}} \quad (6)$$

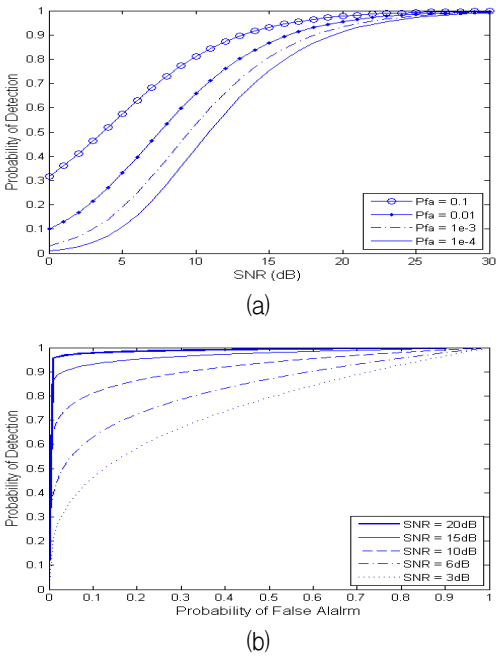

그림 3. (a) SNR 대 검출 확률, (b) ROC 곡선
Fig. 3. (a) Probability of detection versus SNR, (b) Receiver operating characteristic curve.

where $\alpha^2 = \frac{\sigma^2}{\sigma_0^2} = \frac{\sigma_0^2+\sigma_1^2}{\sigma_0^2} = 1 + SNR$ and γ is the ratio of prior probabilities.

Fig. 3. shows the probability of detection versus SNR and ROC curve. Fig. 3(a) provides a quick view impact of varying system requirements on the required SNR. Lowering the false alarm rate results in higher required SNRs for the same probability of detection. Also, if the required probability of detection is reduced while maintaining the same false alarm rate, lower SNRs are required.

For preprocessing, Band pass filter with a center frequency within the frequency band of 10~50 Hz is used for eliminate the power noise(60Hz) and unknown noise(8Hz). For processing the footstep extraction sliding window and background noise adapted threshold are used. Fig. 4 shows the flowchart for the algorithm used in extracting the footsteps form seismic signal. By comparing windowed seismic signal with adaptive threshold, we save data when the location of maximum of absolute value of data is same as the median of data.

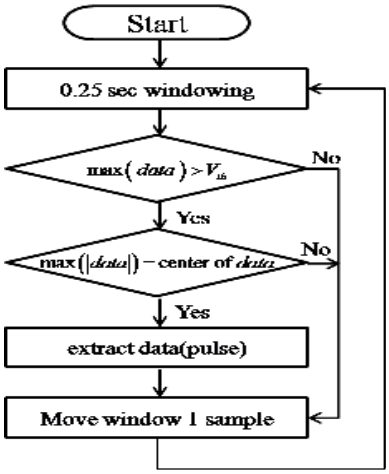

그림 4. 진동신호에서의 발자국 추출을 위한 흐름도
Fig. 4. Flowchart for footstep extraction from seismic signal.

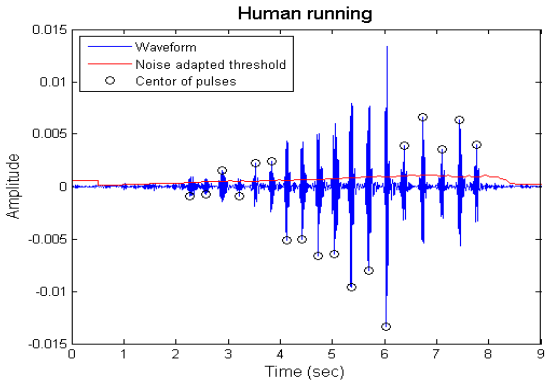

그림 5. 진동신호에서의 발자국 추출
Fig. 5. Footstep extraction from seismic signal.

Window slides one sample and next segment of data is obtained and processed. To guarantee the performance under the variation of background noise, the algorithm updates the scale parameter of background noise every 1000 samples and recalculate the threshold. If the absolute value of background noise is smaller than the initial threshold, then it is accumulated in buffer, and updates the scale parameter. The buffer size of 1000 calculates the distribution of noise in 0.5sec with sampling frequency of 2000Hz. The threshold is updated using calculated scale parameter and the Eq. (4).

Fig. 5 shows the intermediate result of footstep extraction. The blue solid line is the waveform of band pass filtered seismic signal. The red solid line indicates the noise adapted threshold using Eq. (4) under false alarm of 10%. The black circles are the centers of window for extracting footstep. After footstep extraction, all footsteps are normalized by power for feature extraction.

Ⅲ. Feature extraction

1. Spectrum based features

The most common method for frequency analysis is the Fast Fourier transform(FFT). For the first feature vector, we use absolute value of FFT corresponding to 10Hz to 100Hz.

For second feature vector, we use the continuous wavelet transform(CWT) which use wavelet function for frequency representation. The CWT compares the signal to shifted and compressed or stretched versions of a wavelet and is defined as follows:

$$C(a,c;\delta(t-\tau),\psi(t)) = \int_{-\infty}^{\infty}\delta(t-\tau)\frac{1}{\sqrt{\alpha}}\psi^*\left(\frac{t-b}{a}\right)dt = \frac{1}{\sqrt{\alpha}}\psi^*\left(\frac{\tau-b}{a}\right) \quad (7)$$

where $\psi(t)$ is a wavelet function, t is time, and α is scale. The scale values determine the degree to which the wavelet is compressed or stretched. The low scale values compress the wavelet and correlate better with high frequencies. The CWT coefficients at lower scales represent energy in the input signal at higher frequencies, while CWT coefficients at higher scales represent energy in the input signal at lower frequencies. For the feature vector, we use square of CWT coefficients of scale from 10 to 100.better with high frequencies. The CWT coefficients at lower scales represent energy in the input signal at higher frequencies, while CWT coefficients at higher scales represent energy in the input signal at lower frequencies. For the feature vector, we use square of CWT coefficients of scale from 10 to 100.

For third feature, we use autoregressive(AR) spectrum analysis especially using the Burg

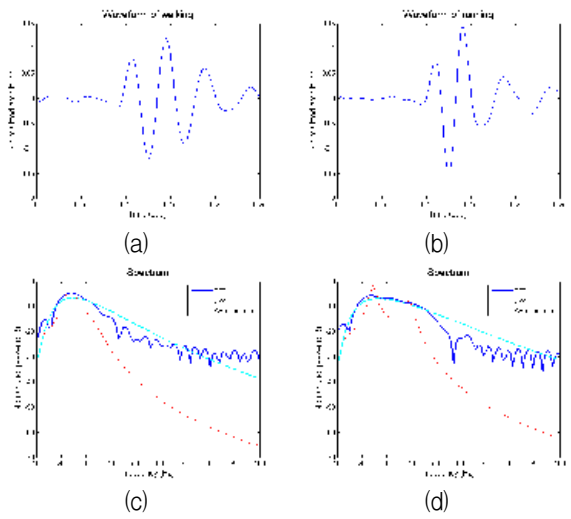

그림 6. 각 발자국 펄스 분석 (a) 걷기의 파형, (b) 뛰기의 파형, (c) 걷기의 주파수 스펙트럼, (d) 뛰기의 주파수 스펙트럼

Fig. 6. Analysis of each footstep pulse. (a) Waveform of walking, (b) Waveform of running, (c) Frequency spectrum of walking, (d) Frequency spectrum of running.

algorithm. The estimate of the power spectral density(PSD) of the signal is used as feature. We use 16th order of AR prediction model for the estimate of PSD. In Fig. 6, we show waveforms and frequency spectrums obtained from FFT, CWT and AR prediction model. The solid blue lines in Fig 6(c) and Fig 6(d) indicate the FFT results of walking and running respectively. We can observe that the impact of running on the ground causes wider frequency band than that of walking. The dashed cyan line in Fig. 6(c) and Fig. 6(d) indicate the frequency spectrum form CWT results when gaussian function('gaus4') is used as wavelet and the resulting output power value for scale is converted to frequency. The dotted lines in Fig. 6(c) and Fig 6(d) indicates the AR spectrum of walking and running respectively. We can notice that the signal from walking has one peak of mid 20Hz, where signal from running has two peak of mid 20Hz and mid 30Hz.

2. AR spectrogram based feature

The footstep signatures of humans or animals obtained using seismic sensors are non-stationary in nature. By using this fact, we employ time-frequency analysis. Time-frequency analysis is to find what frequency occurs at what time in a signal. This is performed by mapping a one dimensional signal in the time domain, into a two dimensional time-frequency representation of the signal. Spectrogram is visualizations of the evolution of the PSD of signal swept through time. For PSD estimation, we use AR spectrum.

Let AR spectrogram image $I(x, y)$ be a two-dimensional $N_1 \times N_2$ array of intensity values. An image may also be considered as a vector of dimensional $N_1 N_2$, so that image in this paper of size 100 by 473 becomes a vector 47300-dimensional space. An ensemble of images, then, maps to a collection points in this huge space. Nevertheless image can be described by a relatively low dimensional subspace. For extract the feature vector in AR spectrogram analysis, we use the eigen-image technique which is widely used in face recognition and image processing area. The eigen-image technique functions by projecting spectrogram images onto a feature space that spans the significant variations among known spectrogram images. The significant features are the eigenvectors of the set of images. The projection operation characterizes an individual spectrogram image by a weighted sum of the eigen-image features, and so to classification a particular spectrogram image it is necessary only to compare these weights to those of known individuals[13]. The goal of AR spectrogram analysis is to extract weights as a feature vector for classification. AR spectrogram are used as the image for the eigen-image. In what follows, describe how to calculate the weight in details.

Let the training set of AR spectrogram images be $\underline{\Gamma}_1, \underline{\Gamma}_2, \ldots, \underline{\Gamma}_M$, each vector is of length $N_1 N_2 \times 1$, describes an $N_1 \times N_2$ image. Each spectrogram differs from the average by the vector $\underline{\Phi}_i = \underline{\Gamma}_i - \underline{\Psi}$, where the average spectrogram of the set is defined by

$\underline{\Psi}=\frac{1}{M}\sum_{n=1}^{M}\underline{\Gamma}_n$. The covariance matrix is Eq. (8).

$$\boldsymbol{C}=\frac{1}{M}\sum_{n=1}^{M}\underline{\Phi}_n\underline{\Phi}_n^{T}=\boldsymbol{A}\boldsymbol{A}^{\boldsymbol{T}} \tag{8}$$

where the matrix $\boldsymbol{A}=[\underline{\Phi}_1\ \underline{\Phi}_2\cdots\underline{\Phi}_M]$. The matrix $\boldsymbol{C}$, however, is $N_1N_2\times N_1N_2$, and determining the N_1N_2 eigenvectors and eigenvalues is an intractable task for typical spectrogram size. If the number of data points in the image space is less than the dimension of space($M<N_1N_2$), there will be only $M-1$, rather than N_1N_2, meaningful eigenvectors. Consider the eigenvector $\underline{v}_i$ of $\boldsymbol{A}\boldsymbol{A}^T$ such that $\boldsymbol{A}\boldsymbol{A}^T\underline{v}_i=\mu_i\underline{v}_i$. Pre-multiplying both side by $\boldsymbol{A}$, we have Eq. (9).

$$\boldsymbol{A}\boldsymbol{A}^{\boldsymbol{T}}\boldsymbol{A}\,\underline{v}_i=\mu_i\boldsymbol{A}\,\underline{v}_i \tag{9}$$

From which we see that $\boldsymbol{A}\underline{v}_i$ are the eigenvectors for $\boldsymbol{C}=\boldsymbol{A}\boldsymbol{A}^{\boldsymbol{T}}$. Following analysis, we construct the $M\times M$ matrix $\boldsymbol{L}=\boldsymbol{A}^{\boldsymbol{T}}\boldsymbol{A}$, where $L_{mn}=\underline{\Phi}_m^T\underline{\Phi}_n$, and find the M eigenvectors, $\underline{v}_i$, of $\boldsymbol{L}$. In practice, a smaller $M'(M'<M)$ is sufficient for identification, since accurate reconstruction of the AR spectrogram image is not a requirement. The eigenimages span an M'-dimensional subspace of the original N_1N_2 image space. In many of our test cases, based on $M=20$ AR spectrogram images, $M'=19$ eigenimages were used. A new AR spectrogram image($\underline{\Gamma}$) is transformed into its eigenimage components by a simple operation,

$$\omega_k=\left(\boldsymbol{A}\,\underline{v}_k\right)^T\left(\underline{\Gamma}-\underline{\Psi}\right) \tag{10}$$

for $k=1,2,\ldots,M'$, The weights from a vector $\underline{\Omega}=[\omega_1\ \omega_2\cdots\omega_{M'}]^T$ hat describes the contribution of each eigen-image in representing the input AR spectrogram image, treating the eigen-images as a basis set for AR spectrogram images. The weight vector may then be used as a feature vector.

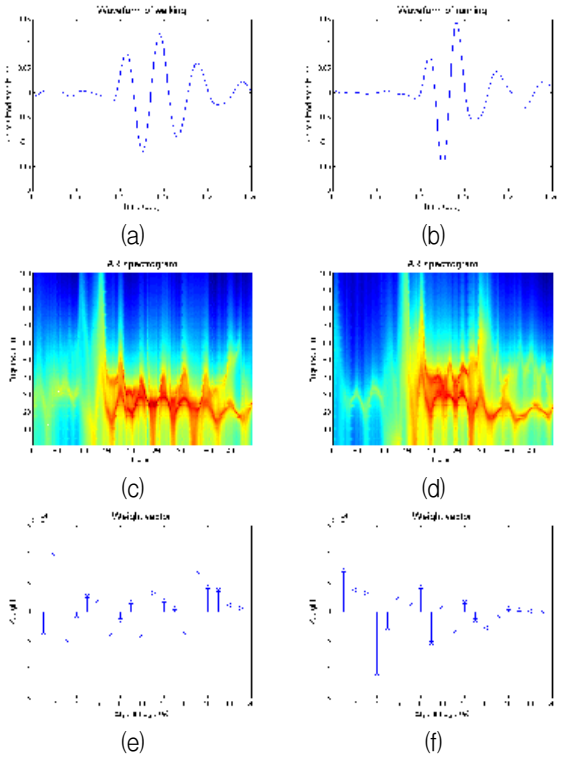

그림 7. 각 발자국 분석 (a) 걷기의 파형, (b) 뛰기의 파형, (c) 걷기의 AR 스펙트로그램, (d) 뛰기의 AR 스펙트로그램, (e) 걷기의 가중치 벡터, (f) 뛰기의 가중치 벡터

Fig. 7. Analysis of each footstep (a) Waveform of walking, (b) Waveform of running, (c) AR spectrogram for walking, (d) AR spectrogram for running, (e) Weight vector of walking. (f) Weight vector of running.

The proposed algorithm uses eigenvalue decomposition and matrix-vector operation. Major computation is eigenvalue decomposition of which computational complexity is $O(M^3)$. Since the $M=20$ in our case, $O(20^3)$ and matrix-vector operation are added for feature extraction.

Fig. 7 shows feature extraction based on AR spectrogram. Fig. 7(c) and Fig. 7(d) indicate the AR spectrogram of walking and running respectively. For AR processing sliding window is used, which size is 32 millisecond and sliding 0.5 millisecond, and next segment of data is obtained and processed. The order of an AR prediction model is 16th order. The weight vectors($\underline{\Omega}$) are indicated in Fig. 7(e) and Fig. 7(f).

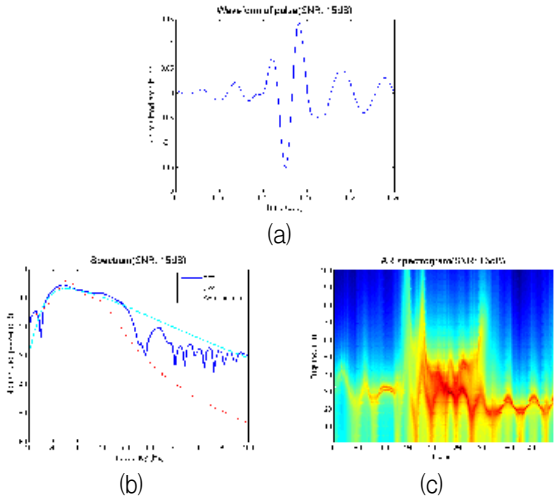

그림 8. 15dB SNR 잡음이 있는 뛰는 발자국에 대한 분석 (a) 파형, (b) 주파수 스펙트럼, (c) AR 스펙트로그램

Fig. 8. Analysis of running footstep with noise, 15dB SNR (a) Waveform, (b) Frequency spectrum, (c) AR spectrogram.

3. Feature comparison in noise environment

In order to compare the change in accuracy for noise, we analyze feature using footstep added white Gaussian noise with various SNR. Fig.7 indicate the spectrum and AR spectrogram of Fig 6(b) added 15dB white Gaussian noise. Fig 6(d) and Fig 8(b) indicate the spectrum of running footstep and that with noise respectively. In comparison with two spectrums, noise has influence on FFT, CWT and AR spectrum, e.g., AR spectrum of clean footstep has 2 peak mid-20 and mid-30 Hz, but AR spectrum of footstep added noise has only one peak in mid-20 Hz. In Fig 7(d) is AR spectrogram of running and AR spectrogram of added 15dB white Gaussian noise is in Fig 8(c). Noise has no direct effect on AR spectrogram until 15dB.

Ⅳ. Classification results

1. Single footstep result

In this section, we present experimental results. In Table 2, we describe the feature vectors for classification. The classification algorithms used in this paper is linear SVM. 10% of data set is used for training, and the rest of data set is used for the performance evaluation test. We evaluate the classification performance of features using FFT, CWT, AR spectrum and AR spectrogram of the seismic footstep dataset.

표 2. 특징 벡터

Table 2. Feature vectors.

Analysis		Feature	Size
Spectrum	FFT	Absolute value of FFT frequency 10~100Hz.	90×1
	CWT	Square of CWT coefficients of 10~100 scale.	90×1
	AR	16th order AR spectrum frequency 10~100Hz.	90×1
Spectrogram	AR	Weight vector from spectrogram image.	19×1

표 3. 제안된 특징벡터를 이용한 분류결과(%) 비교

Table 3. Comparison of the classification accuracy(%) by using proposed feature vector.

Feature	walking	running
FFT	80.95	80.26
CWT	85.71	88.16
AR spectrum	85.71	89.47
AR spectrogram	93.65	97.74

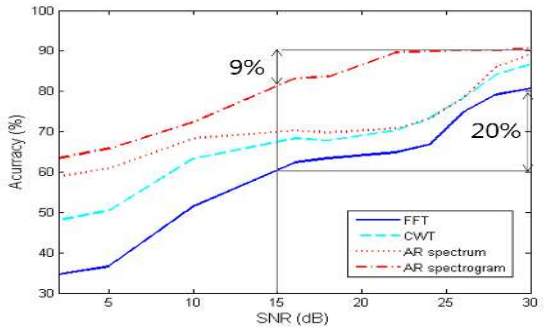

그림 9. SNR에 대한 FFT, CWT, AR 스펙트럼, AR 스펙트로그램의 정확도(%) 비교

Fig. 9. Comparison of accuracy(%) curve for the FFT, CWT, AR spectrum and AR spectrogram with various SNR.

The results of based on spectrum and spectrogram analysis are shown in table 3. In frequency spectrum, the accuracy by using CWT and AR spectrum are roughly 5 to 9% better than FFT. AR spectrum shows the best accuracy result among frequency analysis as 85.71% of walking and 89.47% of running

activities.

Classification accuracy according to various SNR is shown in Fig. 9. These curve indicate that classification accuracy using AR spectrogram is robust against background noise. Performance of AR spectrogram at SNR of 15dB is above 80%, and shows reduction of 9% compared with that at SNR of 30dB. On the other hand, performance obtained from FFT, CWT, and AR spectrum decreases approximately 20%. This indicates that the algorithm based on AR spectrogram is the best in noisy environment.

2. Continuos footsteps result

In practice, human behaviors consist of a sequence of transit activities. If we can reliably classify individual footstep as running and walking, then it would be useful to many applications. In this section, we show the classification of each single step in continuos movement. To demonstrate the performance of the proposed AR spectrogram algorithm, we consider two sequential movement undertaken by person H2 whose height is 171cm and weight is 79kg.

The first movement is obtained when human walk

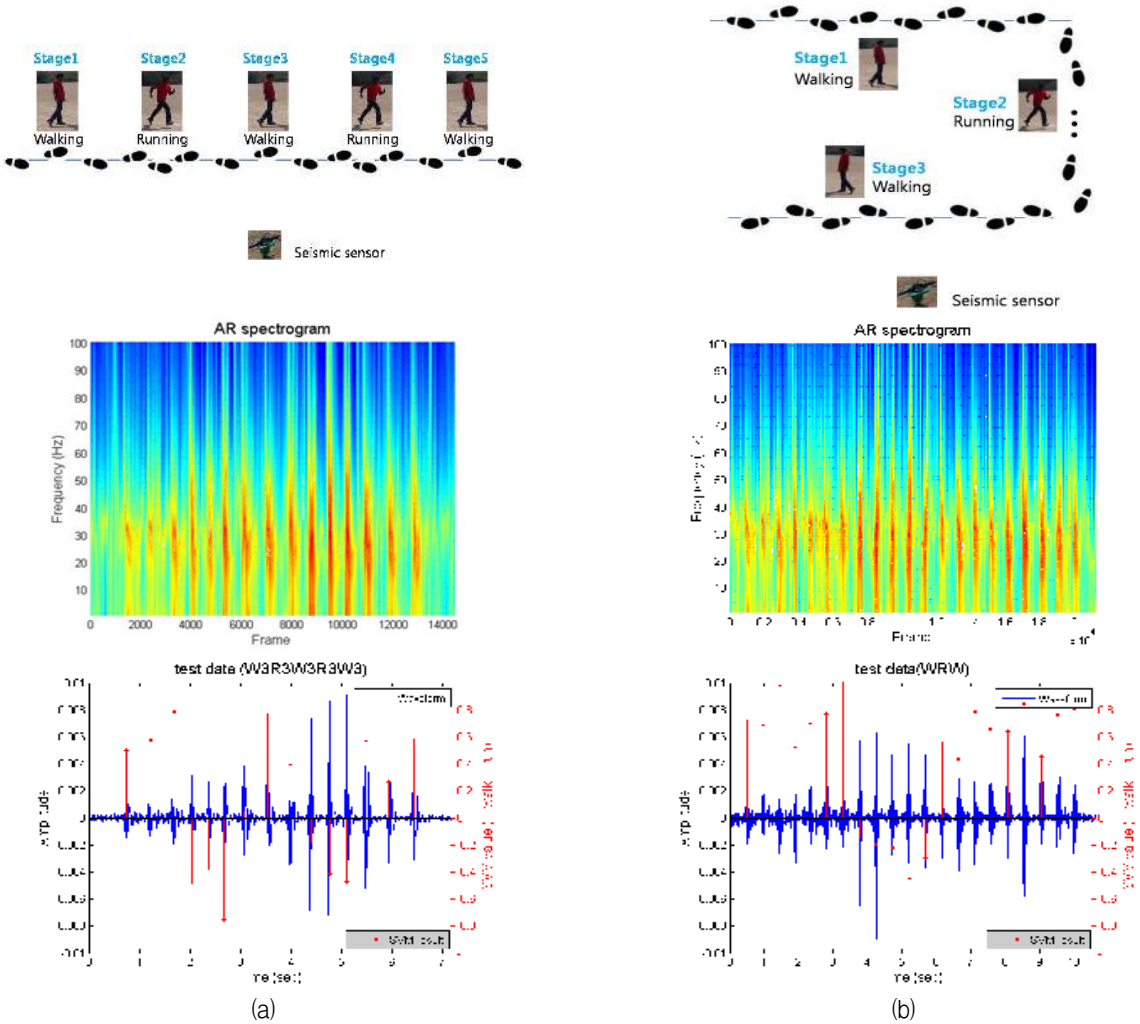

(a) (b)

그림 10. 연속적인 동작의 시나리오, AR 스펙트로그램 및 분류 결과, (a) 첫 번째 시나리오: 걷기3뛰기3걷기3뛰기3걷기3, (b) 두 번째 시나리오: 발자국의 간격이 동일한 걷기, 뛰기, 걷기

Fig. 10. Scenario and AR spectrogram of sequence of activities and their classification results (a) First scenario: W3R3W3R3W3, (b) Second scenario: WRW with same interval of footstep.

three steps and run three steps repeatedly by passing horizontal direction to seismic sensor. The movement path, activities, AR spectrogram, waveform and classification result are shown in Fig 10(a). Also the classification result of SVM is shown as red line. The positive red line represents walking and negative red line represents running. As shown in Fig 10(a), the proposed algorithm detect the each foot step and classify the activity of each step.

The second movement is composed of three movement. The human walks horizontally across the seismic sensor, runs toward seismic sensor and then finally walks across sensor at closer distance.

Note that footstep interval of running is similar to that of walking. The frequency of walking step interval is 1.8 to 2.0 Hz and running step is 2.4 to 3Hz [5],[8] in previous researches. With these algorithms using footstep interval, all step are classified as walking since the estimated step interval frequency is 2.07Hz. However, we can notice that the proposed algorithm can detect the footstep and classify the each activity as shown in the last graph of Fig. 10(b). The first movement and the last movement are classified as walking, and the second movement between two walking movements are classified as running, even the footstep intervals are the same.

The results of two experiments shows the validity and feasibility of the proposed algorithm. Thus the proposed algorithm can be used for human activity detection and classification in complicated and continuos movement.

V. Discussion and conclusion

In this paper, we proposed algorithms for single footstep detection and classification of signal obtained seismic sensor. For footstep detection, we propose an adaptive algorithm using background noise level. The frequency spectrums of FFT, CWT, AR modeling and AR spectrogram are used as feature vector and linear SVM is used for training and classification.

The classification accuracy based on AR spectrogram was found to be 93.65% of walking and 94.74% of running activities. The AR spectrogram based algorithm does not show much classification performance degradation until SNR reaches 15dB. However, algorithms using frequency information show much performance degradation.

Also we showed outstanding movement classification results with two continuous and mixed walking and running data. Even when the footstep interval of running is similar with that of walking, the proposed algorithm shows perfect classification of single footstep. Thus, the proposed algorithm could be a good candidate for determining the single foot step and continuous foot step movement as well.

REFERENCES

[1] D. Raju and D. Ufford, “Personnel detection using ground sensors,” in Defense and Security Symposium, International Society for Optics and Photonics, pp. 656205-656205, Orlando, USA, April 2007.

[2] H. O. Park, A. A. Dibazar, and T. W. Berger, “Protecting military perimeters from approaching human and vehicle using biologically realistic dynamic synapse neural network,” in Proc. of IEEE Conf. on Technologies for Homeland Security, pp. 73-78, Boston, USA, May 2008.

[3] H. O. Park, A. A. Dibazar, and T. W. Berger, “Cadence analysis of temporal gait patterns for seismic discrimination between human and quadruped footsteps,” in Proc. of IEEE International Conf. on in Acoustics, Speech, and Signal Processing, pp. 1749-1752, Taipei, Taiwan, April 2009.

[4] J. Lee, C. H. Lee, J. Bae, J. Kwon, “Target Detection Algorithm Based on Seismic Sensor for Adaptation of Background Noise,” Journal of The Institute of Electronics Engineers of Korea Vol. 50, No. 7, pp. 258-266, July 2013.

[5] J. Lee, J. Bae, C. H. Lee, D. G. Paeng, D. Lee, J. Chun and N. Lee, “Footstep classification of the person movement using seismic sensor,” in Proc. of 7th Conf. on National Defense Technology, Vol. 1, No. 1, pp. 596-602, July 2011.

[6] S. Schumer, “Analysis of human footsteps utilizing multi-axial seismic fusion,” in Acoustics, Speech and Signal Processing (ICASSP), 2011 IEEE International Conference on, pp. 697 - 700, May 2011.
[7] K. M. Houston and D. P. McGaffigan, “Spectrum analysis techniques for personnel detection using seismic sensors,” in Aero Sense, International Society for Optics and Photonics, pp. 162-173, Orlando, USA, September 2003.
[8] T. Damarla, A. Mehmood, J. Sabatier, “Detection of people and animals using non-imaging sensors,” in Proc. of 14th International Conference on Information Fusion, pp. 1-8, Chicago, USA, July 2011.
[9] R. Bland, “Acoustic and seismic signal processing for footstep detection,” Doctoral thesis, Massachusetts Institute of Technology, Dept. of Electrical Engineering and Computer Science, Cambridge, MA, 2006.
[10] G. Succi, D. Clapp, R. Gampert, and G. Prado, “Footstep detection and tracking,” in Proc. of Aerospace/Defense Sensing, Simulation, and Controls, pp. 22-29, Orlando, FL, USA, September 2001.
[11] H. Park, A. Dibazar, and T. Berger, “The application of dynamic synapse neural networks on footstep and vehicle recognition,” in Proc. International Joint Conference on Neural Networks IJCNN 2007, pp. 1842-1846, Atlanta, USA, August 2007.
[12] S. G. Iyengar, P. K. Varshney, and T. Damarla, “On the detection of footsteps based on acoustic and seismic sensing,” in Signals, Systems and Computers, Conference Record of the Forty-First Asilomar Conference on, Pacific Grove, pp. 2248 - 2252, CA, USA, November 2007.
[13] M. Turk, A. Pentland, “Eigenfaces for recognition,” Journal of Cognitive Neuroscience Vol 3, No. 1, pp. 71-86, 1991.

저 자 소 개

강 윤 정(학생회원)
2006년 한국과학기술원(KAIST) 전기 및 전자공학과 학사 졸업.
2014년 제주대학교 해양시스템 공학과 석사 졸업.
2014년~현재 한국과학기술원 (KAIST) 기계항공시스템 공학부 해양시스템공학전공 박사과정.
<주관심분야 : 통계학적 신호처리, 패턴인식, 영상처리>

배 진 호(정회원)
1993년 아주대학교 전자공학과 학사 졸업.
1996년 한국과학기술원(KAIST) 정보통신공학과 석사 졸업.
2001년 한국과학기술원(KAIST) 전자전산학과 박사 졸업.
1993년~2002년 ㈜대양전기공업 실장.
2002년~2002년 한국과학기술원(KAIST) BK21 초빙교수.
2006년~2007년 Texas A&M 방문교수.
2002년~현재 제주대학교 해양시스템공학과 교수.
<주관심분야 : 광신호처리 및 통신, 레이다 및 소나 신호처리, 항해 시스템>

이 재 일(학생회원)
2009년 제주대학교 해양산업공학 전공 학사 졸업.
2011년 제주대학교 해양정보 시스템공학과 석사 졸업.
2011년~현재 제주대학교 해양 시스템공학과 박사과정.
<주관심분야 : 통계학적 신호처리, 센서 신호처리, Parametric Array, 수중통신>

이 종 현(정회원)-교신저자
1985년 한양대학교 전자공학과 학사 졸업.
1987년 Michigan Technological University 석사 졸업.
2002년 한국과학기술원(KAIST) 전기 및 전자공학과 박사 졸업.
1990년~1995년 한국전자통신연구원 선임연구원.
2000년~2002년 ㈜KM Telecom 연구소장.
2003년~2006년 서경대학교 전자공학과 전임강사
2006년~현재 제주대학교 해양시스템공학과 부교수.
<주관심분야 : 통계학적 신호처리, 적응 배열 시스템, 수중 및 이동 통신, UWB 무선전송기술>